Advances in Engineering Research : Possibilities and Challenges
ISSN Print: 3079-5192
ISSN Online: 3079-5206
https://doi.org/10.63313/AERpc.9036

Dynamic analysis of gear rotor system considering shaft bending

Yanan Shi*. Fuhao Liu and Chengxiang Hu
Qingdao University of Technology, Qingdao 266000, China
Email: 948292727@qq.com

How to cite this paper: Shi, Y. N., Liu, F. H., & Hu, C. X. (2025). Dynamic analysis of gear rotor system considering shaft bending. Advances in Engineering Research: Possibilities and Challenges, 2(1), 48-57. ISSN Print: 3079-5192; ISSN Online: 3079-5206.
https://doi.org/10.63313/AERpc.9036
Published: 2025-07-24

Abstract

Considering that shaft bending is one of the most common errors in the manu-facturing of gear shaft systems. Therefore, this should be an important con-sider-ation in the dynamic simulation process. Based on the establishment of the dy-namic model of the spur gear system including shaft bending, the influence of single-bend crankshafts and double-bend crankshafts on the dynamic response of the system was considered. The results show that the greater the degree of shaft bending, the greater the vibration amplitude of the system. Therefore, the degree of shaft bending should be controlled within a reasonable range to pre-vent it from causing instability in the gear system.

Keywords

Gear system; shaft bending; Dynamic analysis

1. Introduction

Rotating machinery is widely used in power generation and transmission projects. In these applications, gear rotor systems are typically used to change speed and/or working direction. With the continuous improvement of people's requirements for high speed and lightweight, the research on the dynamics of gear transmission rotors has become increasingly important. This is because gear-driven rotor systems often have more severe noise and vibration, durability and efficiency issues under high-speed operation conditions, especially when there are manufacturing deviations in components such as shafts. Therefore, studying the dynamic behavior of gear rotor systems with certain axial deviations to gain a deeper understanding of their potential physical properties is helpful for designing and developing quieter and more durable gear rotor systems.

The dynamic behavior of the rotors has been studied for over one century and analysis techniques of rotor dynamics have been fairly well established[1]. Approaches to dynamic analysis of the rotor systems can be divided into three main branches, that is, analytical models, transfer metric method (TMM), and finite element method (FEM). Analytical methods for rotor dynamic analysis were formulated in early models[2]. TMM was first proposed by Prohl[3] and solves rotor dynamic problems in the frequency domain. Later, many researchers[4] continuously developed the TMM and published plenty of articles in the open literature. The dynamic behavior of the geared rotor system is different from typical rotor-bearing system, where lateral and torsional vibrations can be conducted separately. Mitchell and Mellen[5] experimentally studied the dynamic property of the geared rotor system, and their results showed that the coupling effect between lateral and torsional vibrations should not be neglected. This is mainly because of the presence of the gear mesh characteristics in the geared rotor system. Recently, Choi and Mau[6] conducted an analytical study of the dynamic characteristics of a geared rotor-bearing system by the TMM. In their study, they modeled the gear mesh as a pair of rigid disks connected by a spring– damper set. The steady-state response due to the excitation of mass unbalance, geometric eccentricity, and transmission error (TE) was obtained using TMM. Most recently, Q Han et al. [7] studied the dynamic behavior of a geared rotor-bearing system with a breathing slant crack using FEM. These previous research works focus on different aspects of the dynamic characteristics of geared rotor system and lead to improvements in understanding the dynamics of the geared rotor system. The importance of the coupled lateral––torsional vibration modes in geared rotor systems has received increasing attention in the past decade[8]. It has been shown in some studies that the gear–shaft interaction has considerable influence on the gear mesh and bearing responses due to the coupling between gear mesh modes and shaft bending flexibility[9]. As modern geared systems developed to transfer higher load and speed with lighter weight and smaller capacity, the geared system is much more sensitive to excitations from manufacturing deviations, for example, shaft bending deviation. Therefore, evaluation of shaft manufacturing bending deviation on the dynamic behavior of the geared rotor system is needed to be conducted.

The purpose of this paper is to theoretically evaluate the influence of shaft bending deviation on the dynamic characteristics of the gear transmission rotor system. The organization of this article is as follows: The second part aims to establish a dynamic model of shaft bending. Then the dynamics of shaft bending and the mass stiffness damping matrix of the system were derived. The third part analyzes the dynamic behavior of the gear rotor system. Then the conclusion was drawn in the last section.

2. Dynamic modeling

2.1. Calculation of time-varying meshing stiffness of gear

Figure 1 depicts the generalized coordinates of the paired gear pair. The motion of the gear set can be defined in terms of six generalized coordinates, which are assumed to be planar motions, for each gear there are two translational coordinates and one rotational coordinate. The dotted circle and solid circle indicate the gear pairs before and after the motion, respectively. The center of the stationary gear is represented by the nodes O_6, O_{16}, and the initial center distance is L_0. Considering gear translational motions, the axis centers can move to nodes O_6' and O_{16}'. The angle β represents the position of the gear relative to the pinion after motion. The deviation due to axis bending is indicated by ρ_i. φ_0 and φ_1 are the initial eccentricity angles. For simplicity, they are generally assumed to be zeroes at $t = 0s$.

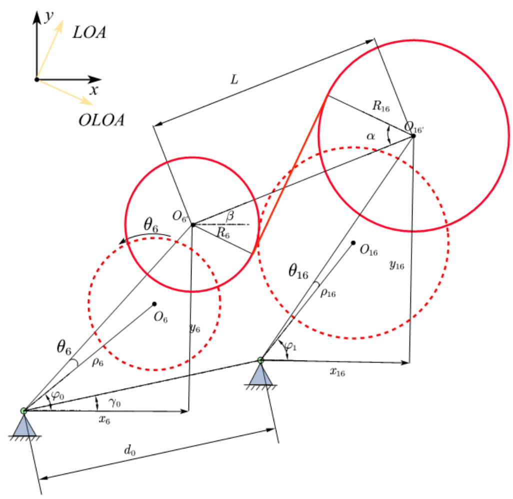

Figure 1. Gear pair variable center distance model.

The vibration displacements of gear i are given by translational coordinates, x_i and y_i, The rotation angle displacements of gear i are given by angular coordinates ϕ_i which can be expressed as follows:

$$\phi_i(t) = \begin{cases} \theta_i(t) + \varphi_0 & i = 1 \sim 10 \\ \theta_i(t) + \varphi_1 & i = 11 \sim 20 \end{cases} \tag{1}$$

where, θ_i is the torsional angle displacement superimposed on the rigid-body rotation of gear i.

Let the rotation direction of pinion is positive, then the displacement vectors of the mass centers G_6, G_{16} in the coordinate systems $O_6x_6y_6$, $O_{16}x_{16}y_{16}$ can be expressed as, respectively.

$$\boldsymbol{r_i} = (x_i - \rho_i \cos\phi_i)\boldsymbol{i} + (y_i - \rho_i \sin\phi_i)\boldsymbol{j} \tag{2}$$

Due to the translational motions of pinion and gear, the gear center distance L_0 is changed to L after the motion. The actual center distance L is given by:

$$L = \sqrt{\left(x_{16} - x_6 + d_0\cos\gamma_0\right)^2 + \left(y_{16} - y_6 + d_0\sin\gamma_0\right)^2} \tag{3}$$

where, x_6 and x_{16} denote the translational displacements of the pinion and large gear in the x-direction, respectively, and y_6 and y_{16} denote the translational displacement of the pinion and large gear in the y-direction, respectively. $d_0 = R_6 + R_{16}$, R_6 and R_{16} denote the pitch circle radius of the pinion and gear, respectively.γ_0 is the angle of the two axes.

The actual pressure angle α is define as the angle between the LOA and the direction of velocity at the pitch node, and can be expressed as: The position angle β can be expressed as:

$$\alpha = \cos^{-1}\frac{R_6 + R_{16}}{L}; \quad \beta = \tan^{-1}\frac{y_{16} - y_6 + d_0 \sin\gamma_0}{x_{16} - x_6 + d_0 \cos\gamma_0} \tag{4}$$

The relative displacement of the gear system δ_O along off-line-of-action ($OLOA$) due to translational motion, and the dynamic transmission error δ along LOA can be expressed as:

$$\delta_O = (x_6 - x_{16})\cos(\alpha - \beta) - (y_6 - y_{16})\sin(\alpha - \beta) \tag{5}$$

$$\delta_L = (x_6 - x_{16})\sin(\alpha - \beta) + (y_6 - y_{16})\cos(\alpha - \beta) + R_6\theta_6 + R_{16}\theta_{16} \tag{6}$$

where, θ_6 is the angular displacement of the pinion, θ_{16} is the angular displacement of the large gear.

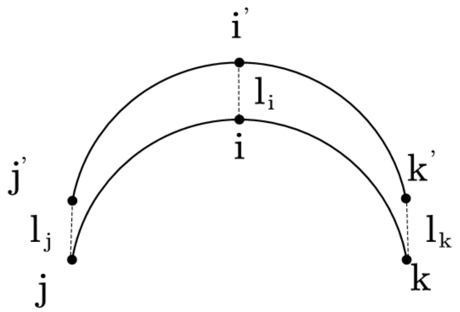

Figure 2 A diagram of a bending shaft segment

2.2 Derivation of the equations of motion

The differential equations of motion for the shaft can be derived by the three generalized coordinates, whose vector form is written as

$$\boldsymbol{X}_i = [x_i,\ y_i,\ \theta_i] \tag{7}$$

The kinetic energy T, potential energy U and dissipation function R of the system in terms of the generalized coordinates can be deduced, respectively.

Analysis was performed at shaft segment without gears or pinion j ~k

The total kinetic energy of the axial segment is：

$$\begin{aligned} \boldsymbol{T}_i = &\left(m_j\left(\|\dot{r}_j\|\right)^2 + J_j\dot{\theta}_j^2\right)/2 + \left(m_i\left(\|\dot{r}_i\|\right)^2 + J_i\dot{\theta}_i^2\right)/2 \\ &+ \left(m_k\left(\|\dot{r}_k\|\right)^2 + J_k\dot{\theta}_k^2\right)/2 \end{aligned} \tag{8}$$

The total potential energy of the axial segment is

$$\boldsymbol{U}_i = \left(\begin{array}{l} k_{xj}\left(r_{xi}-r_{xj}\right)^2 + k_{xi}\left(r_{xk}-r_{xi}\right)^2 + k_{yj}\left(r_{yi}-r_{yj}\right)^2 \\ +k_{yi}\left(r_{yk}-r_{yi}\right)^2 + k_{\theta j}\left(\theta_i-\theta_j\right)^2 + k_{\theta i}\left(\theta_k-\theta_i\right)^2 \end{array} \right) \Big/ 2 \tag{9}$$

The total dissipation function R consists of the dissipation functions of the radial bearing damping and gear mesh damping.

$$R_i = \begin{array}{l} c_{xj}\left(\dot r_{xi}-\dot r_{xj}\right)^2 + c_{xi}\left(\dot r_{xk}-\dot r_{xi}\right)^2 + c_{yj}\left(\dot r_{yi}-\dot r_{yj}\right)^2 \\ +c_{yi}\left(\dot r_{yk}-\dot r_{yi}\right)^2 + c_{\theta j}\left(\dot\theta_i-\dot\theta_j\right)^2 + c_{\theta i}\left(\dot\theta_k-\dot\theta_i\right)^2 \end{array} \Big/ 2 \tag{10}$$

The differential equations of motion are derived using Lagrange's equation, which is given by

$$\frac{d}{dt}\left(\frac{\partial T}{\partial \dot X_i}\right) - \frac{\partial T}{\partial X_i} + \frac{\partial U}{\partial X_i} + \frac{\partial R}{\partial \dot X_i} = Q_i \tag{11}$$

Considering the effect of gravity, the generalized force vector Q for the gear shaft system are given by

$$Q_i = \left(0 \ \ \text{-}m_i g \ \ 0\right)^T \tag{12}$$

Substitute Eqs.(8)–(10)into Eq.(11), the equations of motion of the system can be obtained as.

$$\begin{array}{l} M_i \ddot X_i + K_j\left(X_i - X_j\right) + K_i\left(X_i - X_k\right) + C_j\left(\dot X_i - \dot X_j\right) \\ +C_i\left(\dot X_i - \dot X_k\right) + F'_{mi} + F'_{ki} + F''_{ki} + F'_{ci} + F''_{ci} = Q_i \end{array} \tag{13}$$

M_i is the mass matrix of the system, which can be expressed as:

$$M_i = \begin{bmatrix} m_i & 0 & m_i\rho_i \sin\phi_i \\ 0 & m_i & -m_i\rho_i\cos\phi_i \\ m_i\rho_i\sin\phi_i & -m_i\rho_i\cos\phi_i & J'_i + m_i\rho_i^2 \end{bmatrix} \tag{14}$$

The centrifugal force caused is:

$$F'_{mi} = m'_i\rho_i\dot\theta_i^2 \begin{bmatrix} \cos\phi_i \\ \sin\phi_i \\ 0 \end{bmatrix} \tag{15}$$

K_i is the stiffness coefficient matrix, which can be expressed as:

$$K_i = \begin{cases} \begin{bmatrix} k_{xi} & 0 & 0 \\ 0 & k_{yi} & 0 \\ k_{x_i}\rho_i \sin\phi_i & -k_{y_i}\rho_i \cos\phi_i & k_{\theta i} \end{bmatrix} & \text{else} \\ \text{zero}\begin{pmatrix} 0 & 0 & 0 \end{pmatrix} & i = 10, 20 \end{cases} \tag{16}$$

$$K_j = \begin{cases} \begin{bmatrix} k_{xj} & 0 & 0 \\ 0 & k_{yj} & 0 \\ k_{xj}\rho_i \sin\phi_i & -k_{yj}\rho_i \cos\phi_i & k_{\theta j} \end{bmatrix} & \text{else} \\ \text{zero}\begin{pmatrix} 0 & 0 & 0 \end{pmatrix} & i = 11 \end{cases} \tag{17}$$

where, the structural force caused by stiffness is：

$$F'_{ki} = K_j \left[\begin{pmatrix} -\rho_i \cos\phi_i \\ -\rho_i \sin\phi_i \\ 0 \end{pmatrix} - \begin{pmatrix} -\rho_j \cos\phi_j \\ -\rho_j \sin\phi_j \\ 0 \end{pmatrix} \right] \tag{18}$$

$$F''_{ki} = K_i \left[\begin{pmatrix} -\rho_i \cos\phi_i \\ -\rho_i \sin\phi_i \\ 0 \end{pmatrix} - \begin{pmatrix} -\rho_k \cos\phi_k \\ -\rho_k \sin\phi_k \\ 0 \end{pmatrix} \right] \tag{19}$$

where, $k_{xi} = k_{yi} = 12EI/l_i^3$ is the bending stiffness of the i-segment shaft; $k_{\theta i} = \pi G d_i^4/32 l_i$ is the torsional stiffness of the i-segment shaft; E is the modulus of elasticity; I is the moment of inertia of the axis; G is the modulus of shear elasticity; l_i is the length of the i^{th} segment axis, d_i is the diameter of the i-segment shaft. C_i is the viscous damping matrix of the system, which is normally defined as Rayleigh-type damping can be expressed as:

$$C_i = \begin{cases} \begin{bmatrix} c_{xi} & 0 & 0 \\ 0 & c_{yi} & 0 \\ c_{xi}\rho_i \sin\phi_i & -c_{yi}\rho_i \cos\phi_i & c_{\theta i} \end{bmatrix} & \text{else} \\ \text{zero}\begin{pmatrix} 0 & 0 & 0 \end{pmatrix} & i = 10, 20 \end{cases} \tag{20}$$

$$C_j = \begin{cases} \begin{bmatrix} c_{xj} & 0 & 0 \\ 0 & c_{yj} & 0 \\ c_{xj}\rho_i \sin\phi_i & -c_{yj}\rho_i \cos\phi_i & c_{\theta j} \end{bmatrix} & \text{else} \\ \text{zero}\begin{pmatrix} 0 & 0 & 0 \end{pmatrix} & i = 11 \end{cases} \tag{21}$$

where $c_{xi} = c_{yi} = c_{\theta i} 2 \times \lambda' \times \sqrt{k_{xi} / \left(1/m_i + 1/m_i\right)}$, λ' is the coefficient before damping, $\lambda' = 0.025$.

The resulting damping force is:

$$F'_{ci} = C_j \left[\begin{pmatrix} \rho_i \sin\phi_i \dot{\theta}_i \\ -\rho_i \cos\phi_i \dot{\theta}_i \\ 0 \end{pmatrix} - \begin{pmatrix} \rho_j \sin\phi_j \dot{\theta}_j \\ -\rho_j \cos\phi_j \dot{\theta}_j \\ 0 \end{pmatrix} \right] \tag{22}$$

$$F''_{ci} = C_i \left[\begin{pmatrix} \rho_i \sin\phi_i \dot{\theta}_i \\ -\rho_i \cos\phi_i \dot{\theta}_i \\ 0 \end{pmatrix} - \begin{pmatrix} \rho_k \sin\phi_k \dot{\theta}_k \\ -\rho_k \cos\phi_k \dot{\theta}_k \\ 0 \end{pmatrix} \right] \tag{23}$$

Analysis was performed at shaft segment with gear or pinion j ~k

Then, the mass matrix of the gear or pinion becomes:

$$M'_i = \begin{cases} \begin{bmatrix} m'_i & 0 & m'_i \rho_i \sin\phi_i \\ 0 & m'_i & -m'_i \rho_i \cos\phi_i \\ m'_i \rho_i \sin\phi_i & -m'_i \rho_i \cos\phi_i & J'_i + m'_i \rho_i^2 \end{bmatrix} & i = 6,16 \\ diag\begin{pmatrix} 0 & 0 & 0 \end{pmatrix} & else \end{cases} \tag{24}$$

The F_m is time-varying meshing force, which can be expressed as:

$$F_m = \sum_{n=1}^{\varepsilon} \left[k_m^n f(\delta, b_t) + c_m^n f_1(\delta, b_t) \right] \tag{25}$$

where, ε denotes the number of teeth engaged at the same time during the meshing process, k_m^n and $c_m^n = 2\xi_m \sqrt{k_m^n J_1 J_2 / (J_1 R_2^2 + J_2 R_1^2)}$ is the mesh stiffness and damping of n^{th} pair of teeth engages respectively.[8] ξ_m is the damping ratio(0.03~0.17); $f(\delta, b_t)$ and $f_1(\delta, b_t)$ are nonlinear functions of tooth clearance and relative velocity, respectively.

$$f(\delta, b_t) = \begin{cases} \delta - \text{sign}(\delta) b_t & |\delta| > b_t \\ 0 & \text{else} \end{cases} \tag{26}$$

$$f_1(\delta, b_t) = \begin{cases} \dot{\delta} - \text{sign}(\delta) \dot{b}_t & |\delta| > b_t \\ 0 & \text{else} \end{cases} \tag{27}$$

$$\begin{aligned} \dot{\delta}(t) = {} & (\dot{x}_6 - \dot{x}_{16}) \sin(\alpha - \beta) + (\dot{y}_6 - \dot{y}_{16}) \cos(\alpha - \beta) + \dot{\theta}_6 R_6 \\ & + \dot{\theta}_{16} R_{16} - \frac{\delta_O}{L \sin\alpha} \left[(\dot{x}_6 - \dot{x}_{16}) \cos(\alpha - \beta) - (\dot{y}_6 - \dot{y}_{16}) \sin(\alpha - \beta) \right] \end{aligned} \tag{28}$$

In order to ensure the formation of normal lubricating oil film between tooth surfaces and prevent gear teeth from getting stuck due to thermal expansion deformation caused by the increase of gear operating temperature, an appropriate gear backlash should be considered. According to, dynamic half backlash due to dynamic changing of axle center distance can be derived as:

$$b_t(t)=b_0+(R_6+R_{16})(\mathrm{inv}(\alpha)-\mathrm{inv}(\alpha_0)) \tag{29}$$

$$\dot{b}_t=\left[(\dot{x}_{16}-\dot{x}_6)\cos\beta+(\dot{y}_{16}-\dot{y}_6)\sin\beta\right]\sin\alpha \tag{30}$$

where, b_0 is the initial backlash, α_0 denotes the initial pressure angle for the initial center distance L_0. The α_0 is generally equal to 20°When the gear pair is perfectly mounted.

The external loads at the 1st and 11th particles also include the input and output torques of the system. The 6th and 16th masses coincide with the pinion and the large gear, respectively, and thus:

$$F_i=\begin{cases}\begin{pmatrix}0\\-(m_i+m_i')g\\0\end{pmatrix}-(F'_{mi}+F'_{ki}+F''_{ki}+F'_{ci}+F''_{ci})-F_m & i=6,16\\ \begin{pmatrix}0\\-m_ig\\T_i\end{pmatrix}-(F'_{mi}+F'_{ki}+F''_{ki}+F'_{ci}+F''_{ci}) & i=1,11\\ \begin{pmatrix}0\\-m_ig\\0\end{pmatrix}-(F'_{mi}+F'_{ki}+F''_{ki}+F'_{ci}+F''_{ci}) & \text{else}\end{cases} \tag{31}$$

3. The influence of bow shaft on the system

During the manufacturing process of shafts, bending is inevitable due to processing or casting and other reasons. On the basis of considering the constant bearing stiffness, the influences of different maximum bending values on the dynamic response of the gear system were compared respectively. The vibration response results under the system's health axis and the bending axis are shown in Figure 3. This section utilizes the time course diagram of DTE to study the influence of bending on the dynamic response of the gear system. According to the parameters in Table 1, when the bending values of the pinion shaft are set to 0.01mm respectively and compared with the healthy shaft (i.e., the bending rate is 0), it can be found that when the bending value of the pinion is 0, the system DTE is a stable periodic motion.

Figure 4 shows the vibration response results of pinion gears with only different bending values. The bending values of the pinion shaft are set to 0.01mm, 0.03mm, and 0.05mm respectively for comparison. It can be found that when considering shaft bending, the imbalance of inertial force within the meshing period will cause fluctuations in the dynamic response of the system due to the existence of the external eccentric inertial force. The dynamic transmission error curve oscillates significantly, but the variation laws of the two curves are the same. The fluctuation range and amplitude of the DTE cycle increase with the increase of the bending value, but the fluctuation trend is basically the same. If the bending is only on the pinion, the number of rotation periods should be an integer multiple of the number of teeth on the pinion.

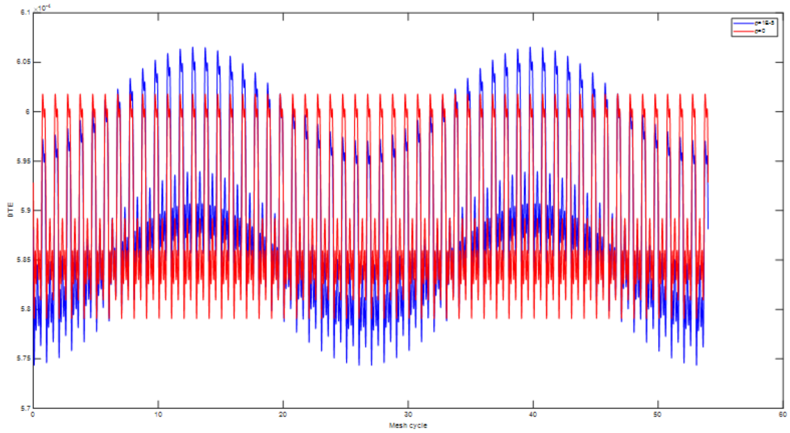

Figure 3. Comparison of DTE time-domain vibration responses between health and bending shafts(red: healthy shaft; bule: shaft bending)

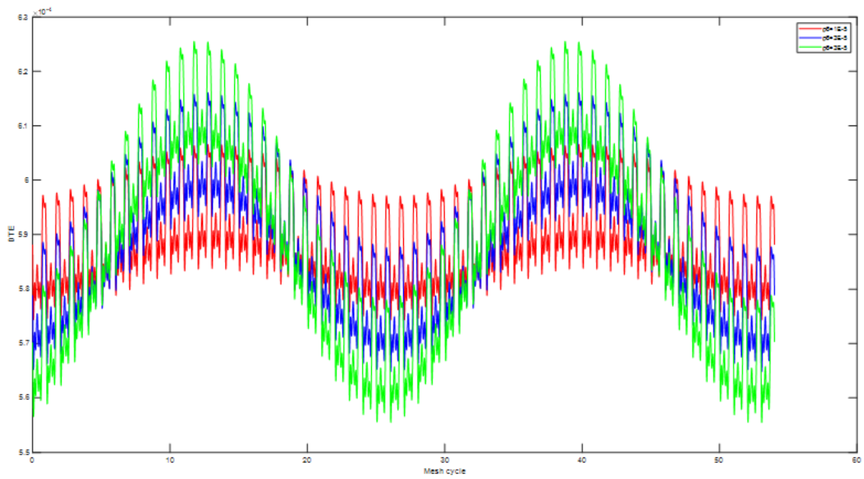

Figure 4. Time-domain vibration responses of DTE with different degrees of shaft bending. (green:$\rho_6 = 0.05mm$; blue:$\rho_6 = 0.03mm$; red:$\rho_6 = 0.01mm$)

Figure 5 shows the vibration response result of the gear with both shafts bent. Set the bending values of both the large and small gear shafts to 0.01mm. When considering biaxial bending, the dynamic response of the system will experience more complex fluctuations, which may lead to further instability of the system. The number of rotation periods is no longer an integer multiple of the number of teeth on the pinion, but the least common multiple of the number of teeth on the large gear and the pinion.

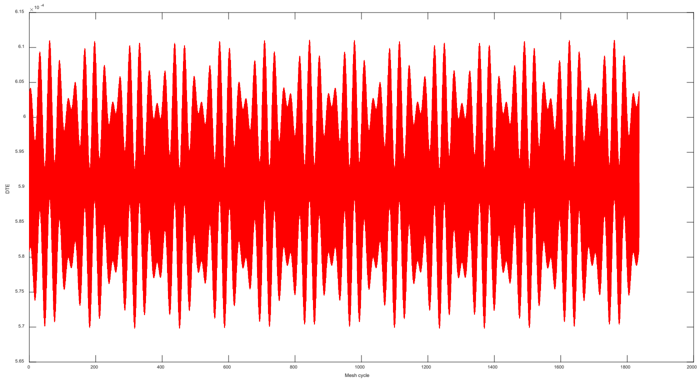

Figure 5. The time-domain vibration response of double-shaft bending

4. Conclusion

The main consideration was the influence of bending on the gear rotor system. The most commonly used six-degree-of-freedom typical dynamic model was established. The dynamic equation of the system was given according to Newton's second law, and the influence of axial bending on the system was discussed under the given single-tooth and double-tooth stiffness of rectangular waves. The results show that when the bending value is zero, the system DTE is a stable periodic motion. When considering shaft bending, due to the existence of eccentric external inertial force, the imbalance of inertial force within the meshing period will cause fluctuations in the dynamic response of the system. The fluctuation range and amplitude of the DTE cycle increase with the increase of eccentricity, but the fluctuation trend is basically the same. When there are multiple faults in the system (double-shaft bending), the system will have more complex vibration responses.

References

[1] Genta G. Dynamics of rotating systems. New York: Springer, 2007.

[2] Dimentberg FM. Flexural vibrations of rotating shafts. London: Butterworths, 1961.

[3] Prohl MA. A general method for calculating critical speeds of flexible rotors. J Appl Mech-T ASME 1945; 12: A142–A148.

[4] Lund JW. Stability and damped critical speeds of a flexible rotor in fluid-film bearings. J Manuf Sci Eng 1974; 96: 509–517.

[5] Mitchell LD and Mellen DM. Torsional-lateral coupling in a geared high-speed rotor system. Mech Eng 1975; 97: 95.

[6] Choi ST and Mau SY. Dynamic analysis of geared rotor bearing systems by the transfer matrix method. J Mech Des 2001; 123: 562–568.

[7] Han Q, Zhao J and Chu F. Dynamic analysis of a geared rotor system considering a slant crack on the shaft. J Sound Vib 2012; 331: 5803–5823.

[8] Li M, Hu HY, Jiang PL, et al. Coupled axial-lateral torsional dynamics of a rotor-bearing system geared by spur bevel gears. J Sound Vib 2002; 254: 427–446.

[9] Yang J and Lim TC. Influence of propeller shaft bending vibration on drivetrain gear dynamics. Int J Auto mot Tech 2015; 16: 57–65.